










Yield degradation due to laser drive asymmetry in D³He backlit proton radiography experiments at OMEGA

Cite as: Rev. Sci. Instrum. **92**, 043551 (2021); <https://doi.org/10.1063/5.0043004>
 Submitted: 05 January 2021 . Accepted: 31 March 2021 . Published Online: 23 April 2021

 T. M. Johnson,  A. Birkel, H. E. Ramirez,  G. D. Sutcliffe,  P. J. Adrian,  V. Yu. Glebov,  H. Sio,  M. Gatu Johnson,  J. A. Frenje,  R. D. Petrasso, and C. K. Li

COLLECTIONS

Paper published as part of the special topic on [Proceedings of the 23rd Topical Conference on High-Temperature Plasma Diagnostics](#)



View Online



Export Citation



CrossMark

ARTICLES YOU MAY BE INTERESTED IN

[An x-ray penumbral imager for measurements of electron-temperature profiles in inertial confinement fusion implosions at OMEGA](#)

Review of Scientific Instruments **92**, 043548 (2021); <https://doi.org/10.1063/5.0041038>

[Phase-field modeling of wetting and balling dynamics in powder bed fusion process](#)

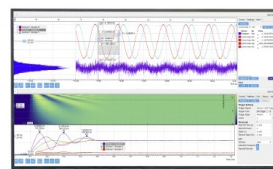
Physics of Fluids **33**, 042116 (2021); <https://doi.org/10.1063/5.0046771>

[Target heating in femtosecond laser-plasma interactions: Quantitative analysis of experimental data](#)

Physics of Plasmas **28**, 023101 (2021); <https://doi.org/10.1063/5.0035356>

Challenge us.

What are your needs for periodic signal detection?



Zurich Instruments

Yield degradation due to laser drive asymmetry in D³He backlit proton radiography experiments at OMEGA

Cite as: Rev. Sci. Instrum. 92, 043551 (2021); doi: 10.1063/5.0043004

Submitted: 5 January 2021 • Accepted: 31 March 2021 •

Published Online: 23 April 2021



View Online



Export Citation



CrossMark

T. M. Johnson,^{1,a)} A. Birkel,¹ H. E. Ramirez,¹ G. D. Sutcliffe,¹ P. J. Adrian,¹ V. Yu. Glebov,² H. Sio,³
M. Gatu Johnson,¹ J. A. Frenje,¹ R. D. Petrasso,¹ and C. K. Li¹

AFFILIATIONS

¹Massachusetts Institute of Technology, Cambridge, Massachusetts 02139, USA

²Laboratory for Laser Energetics, University of Rochester, Rochester, New York 14623, USA

³Lawrence Livermore National Laboratory, Livermore, California 94550, USA

Note: Paper published as part of the Special Topic on Proceedings of the 23rd Topical Conference on High-Temperature Plasma Diagnostics.

^{a)}Author to whom correspondence should be addressed: tmarkj@mit.edu

ABSTRACT

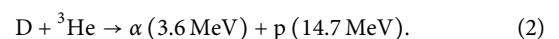
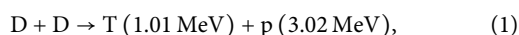
Mono-energetic proton radiography is a vital diagnostic for numerous high-energy-density-physics, inertial-confinement-fusion, and laboratory-astrophysics experiments at OMEGA. With a large number of campaigns executing hundreds of shots, general trends in D³He backlighter performance are statistically observed. Each experimental configuration uses a different number of beams and drive symmetry, causing the backlighter to perform differently. Here, we analyze the impact of these variables on the overall performance of the D³He backlighter for proton-radiography studies. This study finds that increasing laser drive asymmetry can degrade the performance of the D³He backlighter. The results of this study can be used to help experimental designs that use proton radiography.

Published under license by AIP Publishing. <https://doi.org/10.1063/5.0043004>

I. INTRODUCTION

Mono-energetic proton radiography is an essential diagnostic for a number of impactful studies in the area of high-energy-density-physics. Proton radiography¹ enables the study of electromagnetic fields² and warm-dense-matter stopping power³ in laser produced plasmas at OMEGA and on the National Ignition Facility (NIF). It has allowed researchers to explore the kinking behavior of the Crab Nebula jet,⁴ visualize the fields inside and outside an inertial-confinement-fusion (ICF) implosion,⁵ see the fields inside indirect drive hohlraums,⁶ and detect collisionless shocks driven by fast plasma flows.⁷ Numerical methods have recently been applied to proton radiography, enabling the reconstruction of path integrated electromagnetic fields present in the plasma.⁸

Proton radiography implodes a capsule (also called a backlighter) filled with deuterium and helium-3 fuel to produce protons at two specific energies through the nuclear reactions shown in the following:



Note that the energies of the protons are not exactly the same as their birth energies. The protons are born while the laser is still causing the proton energies to be upshifted.¹ These protons will travel through a subject plasma where they are deflected by electromagnetic fields and Coulomb collisions.⁹ The protons are collected using a CR39 nuclear track detector.¹⁰ Etching in NaOH reveals the particle tracks and brings forth the radiograph.

Over the past four years, we have supported over 300 deuterium helium-3 (D³He) backlighter shots at OMEGA from more than 40 experimental shot days. This paper analyzes these shots to find how experimental parameters affect the performance of the D³He backlighter.

The finding of this work is that laser drive asymmetry on the D³He backlighter can affect performance. For a given laser energy, increasing the asymmetry of the laser drive degrades the DD and D³He proton yields. Low laser energy and large asymmetry could compromise the quality of the proton radiographs.

This paper is organized as follows: Section II discusses the experimental parameters in the analysis dataset. The subject of laser drive asymmetry will be discussed in some detail. Section III shows power-law fits of experimental parameters to DD and $D^3\text{He}$ proton yields. A subset of the shots chosen to isolate capsule conditions shows that yields are affected by asymmetry. Section IV summarizes the study and offers experimental design suggestions for proton radiography experiments.

II. EXPERIMENTAL PARAMETERS AND OBSERVABLES

The performance of the $D^3\text{He}$ backlighter can be quantified by measuring the DD and $D^3\text{He}$ proton yields. For the purpose of the present work, the DD proton yield is inferred from the DD neutron yield measured by the neutron time of flight detectors (nTOFs) at OMEGA.¹¹ The $D^3\text{He}$ proton yield is inferred from reactivity scaling¹² using the ion temperature measured by the nTOFs. Yields that are too low can cause very few proton tracks on the CR39, resulting in low quality radiographs. The exact lower bound on the acceptable proton yield will depend on factors such as magnification. For this study, we take the boundary between acceptable and unacceptable proton yields to be 1×10^8 . Figure 1 shows histograms of the DD and $D^3\text{He}$ proton yields. Note that a few of the $D^3\text{He}$ proton yields for the dataset are below the threshold for good radiography data. For some experiments with strong fields and/or high density, the $D^3\text{He}$ proton radiograph can provide cleaner and higher quality data than the DD proton radiographs. This is because the $D^3\text{He}$ proton has higher energy and is therefore stiffer than the lower energy DD proton. The DD proton radiograph is more likely to be washed out if the fields are strong enough to cause particle trajectories to cross. Hence, some shots that have low $D^3\text{He}$ proton yields can compromise the success of an experiment.

A number of experimental parameters contribute to the performance of the $D^3\text{He}$ backlighter for proton radiography. Capsule conditions such as capsule outer diameter, capsule shell thickness, capsule shell roughness, capsule D_2 pressure, and capsule ^3He pressure are determined for each shot. Laser conditions such as laser energy, laser focusing, and laser drive asymmetry are also determined for each shot. The dataset for this study includes all these parameters.

The capsules are normally $420 \mu\text{m}$ in outer diameter. This capsule size was found to result in a small source size needed for radiography to resolve small scale structures.¹ Because these capsules are not the main experimental subject of the experiment, the quality of the capsules is not a priority during target manufacturing. Capsules, therefore, will tend to have variations in capsule outer diameter, shell thickness, and shell roughness. Similarly, the laser conditions on the backlighter are not of the highest quality. Typically, no phase plates or smoothing by spectral dispersion¹³ (SSD) is used to illuminate the backlighter. Both laser and capsule conditions contribute to relatively large shot-to-shot yield variations from the $D^3\text{He}$ backlighter.

Experimental constraints can result in anisotropic illumination of the $D^3\text{He}$ backlighter. Beams are often blocked by targets or other objects in the target chamber. The laser beams used to illuminate the backlighter are typically the leftover beams. Beams that illuminate other targets are chosen first. Changes in the experimental configuration during the shot day further add to beam constraints because

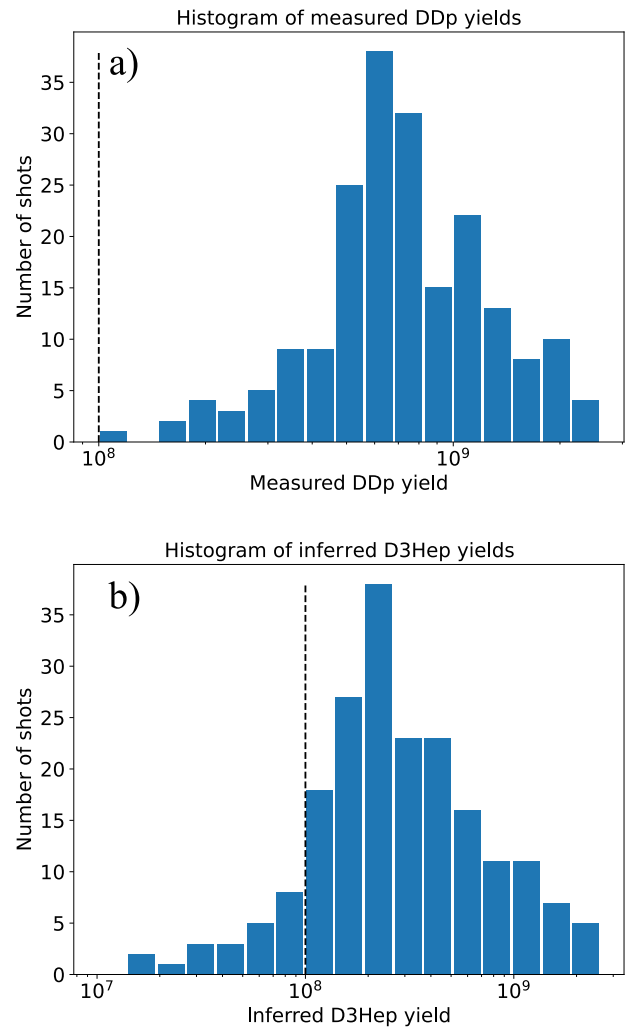


FIG. 1. Summary of the proton yields from the dataset. (a) Histogram of the DD proton yields. (b) Histogram of the inferred $D^3\text{He}$ proton yields. The black dashed line shows the 10^8 yield boundary under which the radiograph quality can be questionable. Note that some of the shots have $D^3\text{He}$ proton yields below this boundary.

repointing beams to the backlighter costs time and could delay shots. All these factors combine to make the laser illumination of the $D^3\text{He}$ backlighter typically asymmetric.

Laser drive asymmetry needs to be quantified in order to observe its impact on DD and $D^3\text{He}$ proton yields. For a given laser configuration, VISRAD¹⁴ is used to generate a laser illumination map. This describes the laser intensity on the backlighter as a function of polar and azimuthal angle. Let this illumination map be $f(\theta, \phi)$. A spherical harmonic decomposition gives a set of expansion coefficients for this function,

$$f_{\ell m} = \int_0^{2\pi} d\phi \int_0^\pi d\theta \sin(\theta) f(\theta, \phi) Y_{\ell m}(\theta, \phi). \quad (3)$$

Summing these expansion coefficients normalized to the average laser power on the target gives the asymmetry

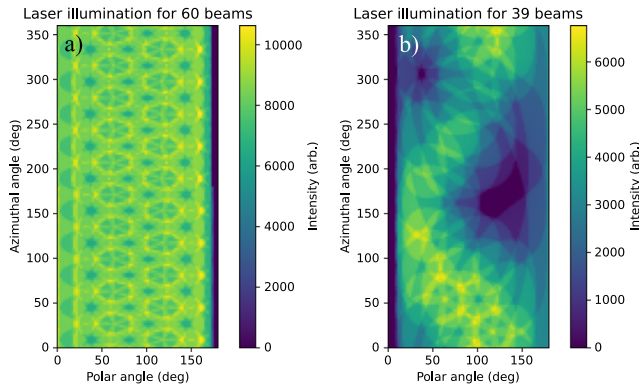


FIG. 2. Laser illumination maps generated from VISRAD. (a) 60 beam configuration at OMEGA. (b) 39 beam configuration. The laser focus conditions are the same for both images. The asymmetry measure for (a) was 0.06, and the asymmetry measure for (b) was 0.44.

measure A ,

$$A^2 = \sum_{\ell=1}^{\ell_{\max}} \sum_{m=-\ell}^{\ell} \left(\frac{f_{\ell m}}{f_{00}} \right)^2. \quad (4)$$

For each ℓ , there are $2\ell + 1$ expansion coefficients. The expansion grows as ℓ^2 , making high mode expansions expensive. This study used an ℓ_{\max} of 10.

Figure 2 shows a comparison between a 60 beam backlighter illumination map and a 39 beam backlighter illumination map. No phase plates are used in either configuration, and the laser focus is the same. Mounting stalks cause the blank region at 180 polar degrees for the 60 beam configuration and the blank region at 0 polar degrees for the 39 beam configuration. Note that there are regions of the 39 beam illumination map that receive no laser light. One would expect that the asymmetry measure would be larger for the 39 beam configuration than that for the 60 beam configuration. Applying the method described above, the asymmetry measure of the 60 beam configuration is found to be 0.06, and the asymmetry measure for the 39 beam configuration is found to be 0.44.

III. ANALYSIS

Trends can be extracted from the dataset of many capsule and laser conditions. A good method for exposing trends in the data is to use a simple power-law model. A least-squares^{15,16} method was used to fit the model,

$$Y_{\text{DDp}} = a \times (\text{OD})^b \times (\Delta R)^c \times (E)^d \times (F)^e \times (A)^f \times (p_{\text{tot}})^g \times (R_p)^h \times (C_r)^i, \quad (5)$$

$$Y_{\text{D}^3\text{He}_p} = a' \times (\text{OD})^{b'} \times (\Delta R)^{c'} \times (E)^{d'} \times (F)^{e'} \times (A)^{f'} \times (p_{\text{tot}})^{g'} \times (R_p)^{h'} \times (C_r)^{i'} \quad (6)$$

to the DD and D³He proton yields, respectively. Here, OD is the capsule outer diameter; ΔR is the capsule shell thickness; E is the laser energy on the capsule; F is the focus offset of the laser; A is the asymmetry measure of the laser illumination; p_{tot} is the total capsule

pressure; R_p is the pressure ratio between ³He and D₂; and C_r is the capsule roughness. The power-laws are fit to all known parameters.

The result of the power-law fits for both DD and D³He proton yields is shown in Fig. 3. The power-law fit for the DD proton yield

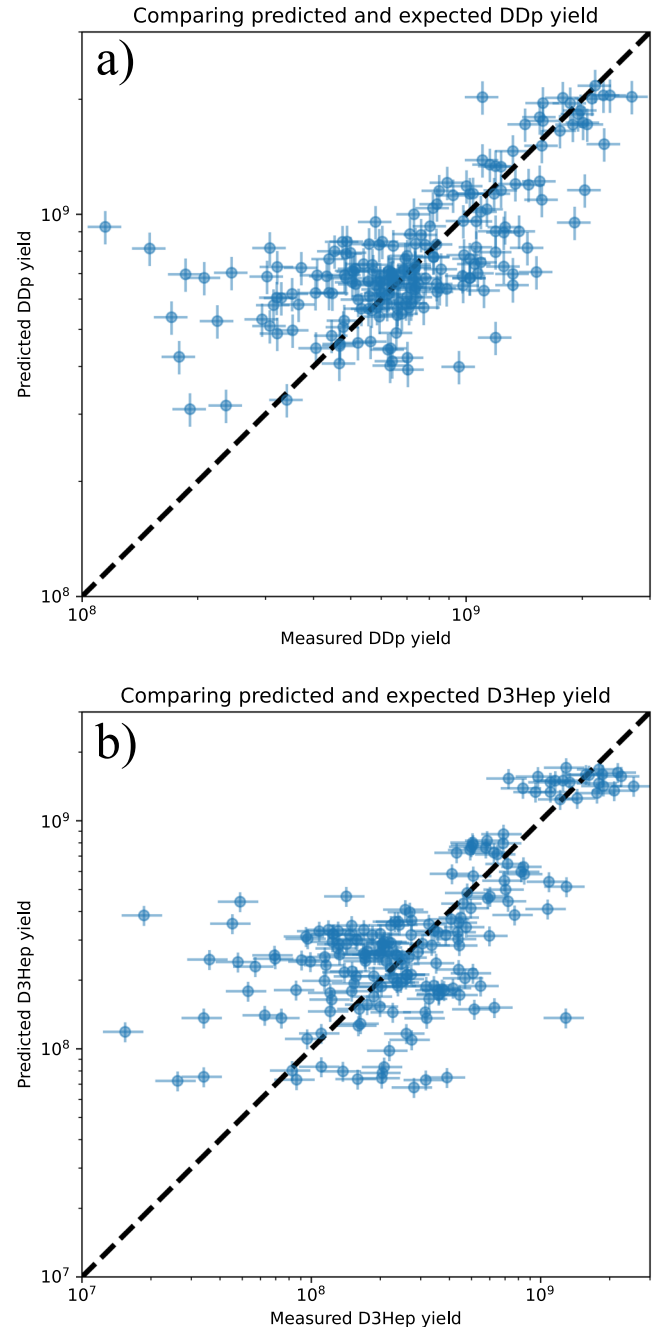


FIG. 3. Least squares power-law fits of the DD and D³He proton yields compared to observed yields. The dashed line shows when the power-law yield is the same as the observed yield. (a) shows this for the DD protons, and (b) shows this for the D³He protons.

TABLE I. Range of parameters and their significance for the DDp and D³Hep power-law fit. The magnitude of the scaling is the ratio of the maximum and minimum values of a parameter raised to the absolute value of the power-law coefficient for that variable.

Parameter	Min value	Max value	Power-law value		Magnitude	
			DDp	D ³ Hep	DDp	D ³ Hep
OD (μm)	387.6	440.1	2.54	2.21	1.38	1.32
ΔR (μm)	1.7	2.4	0.59	0.70	1.23	1.27
E (kJ)	4.38	19.1	0.64	1.46	2.57	8.60
F (μm)	1.6	1.89	0.40	-1.44	1.07	1.27
A	0.151	0.957	-0.68	-1.22	3.51	9.51
p_{tot} (atm)	17.5	21.3	2.19	-1.22	1.51	1.37
R_p	1.875	2.344	1.37	1.80	1.36	1.49
C_r (μm)	0.05	0.85	0.06	0.09	1.19	1.29

does a good job for most of the shots. Most shots have a predicted yield within a factor of two of the measured proton yield. The fit to the D³He proton yield data is not as good as the DD proton yield fit but is good enough to capture the trends in the data. Most shots are within a factor of three of the inferred D³He proton yield. Recall

that these implosions do not use the highest quality capsule or laser conditions. Spread in the proton yields is, therefore, expected. The best fit power-laws are shown as follows:

$$Y_{\text{DDp}} = 9.77 \times 10^{-4} \times (\text{OD})^{2.54} \times (\Delta R)^{0.59} \times (E)^{0.64} \times (F)^{0.40} \times (A)^{-0.68} \times (p_{\text{tot}})^{2.10} \times (R_p)^{1.37} \times (C_r)^{0.06}, \quad (7)$$

$$Y_{\text{D}^3\text{Hep}} = 1.17 \times 10^{-2} \times (\text{OD})^{2.21} \times (\Delta R)^{0.70} \times (E)^{1.46} \times (F)^{-1.44} \times (A)^{-1.22} \times (p_{\text{tot}})^{1.60} \times (R_p)^{1.80} \times (C_r)^{0.09}. \quad (8)$$

Note that these power-law equations should not be extrapolated outside the range of experimental parameters present in the dataset. It would be incorrect to assume that, for example, moving the focus offset as close as possible to the capsule would result in a very large yield. Therefore, the power-law equations are only good approximations within the range of the experimental parameters present in the dataset. The power-law coefficients need to be considered in the context of the range of parameters (see Table I for the magnitude of the scaling for each parameter). Also note that these power-law fits are not meant to allow one to predict the yield of the D³He backlighter. The goal of the fits is instead to observe trends present in the data.

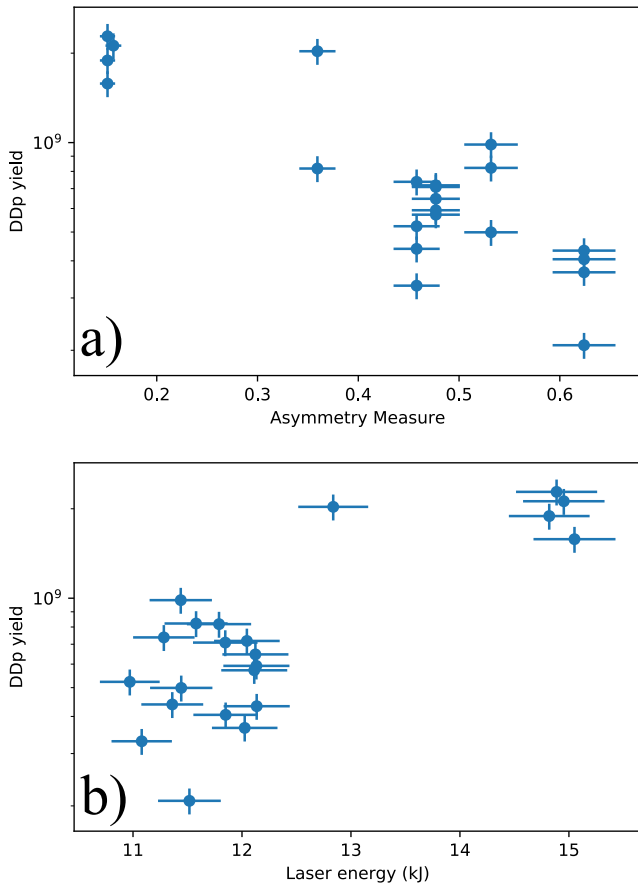


FIG. 4. DD proton yield trends with (a) asymmetry measure and (b) laser energy.

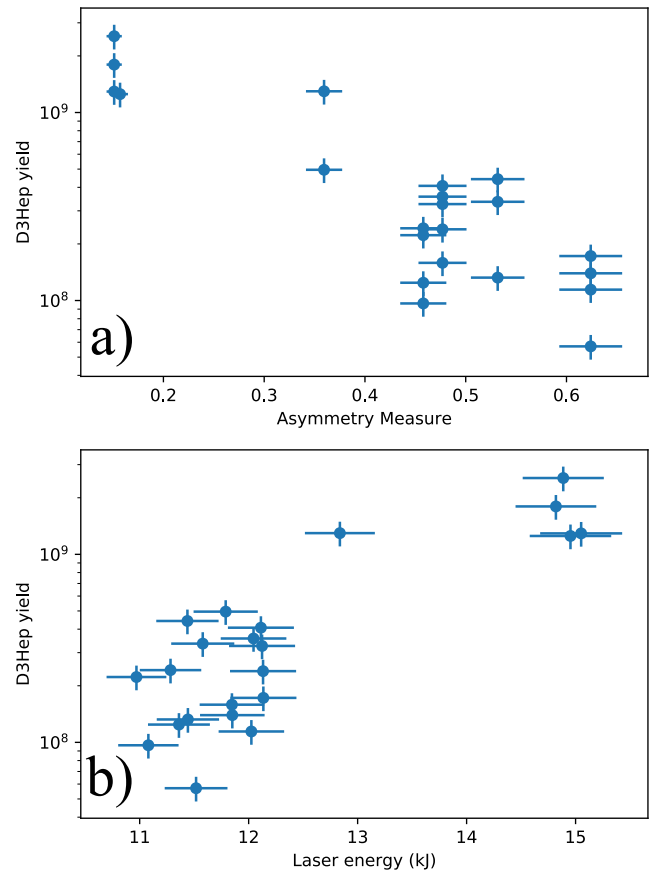


FIG. 5. D³He proton yield trends with (a) asymmetry measure and (b) laser energy.

The power-law fits suggest two important trends. More asymmetry in the laser drive leads to a lower predicted yield. More laser energy leads to a higher predicted yield. To more closely examine the impact of asymmetry, a subset of shots with similar capsule conditions is studied.

Figure 4(a) shows the DD proton yield as a function of asymmetry. The shots shown here were selected to have similar capsule outer diameters and capsule shell thicknesses, as well as a moderate number of beams. This figure shows a clear decrease in yield with increasing asymmetry. Controlling the other experimental parameters lets us conclude that laser drive asymmetry degrades backlighter performance. Figure 5 shows the same but for the D^3He proton yield. The same trends are clear here: asymmetry degrades the yield while laser energy improves the yield. Note that a few of the higher asymmetry D^3He proton yields are below the threshold for good radiography data. This shows that asymmetry can cause a shot to produce a radiograph of questionable quality.

IV. CONCLUSION

Collecting experimental parameters from over 300 D^3He backlighter shots has enabled a unique opportunity to observe the performance of the backlighter for proton radiography at OMEGA. Parameters such as capsule outer diameter, capsule shell thickness, capsule shell roughness, capsule pressure, number of beams on the backlighter, laser energy, laser focusing, and laser drive asymmetry were collected for each shot. Fitting a power-law model to a subset of these parameters revealed trends in the data. The most important predictors of backlighter performance were found to be total laser energy on the capsule and the asymmetry of the laser drive. Down selecting shots to control capsule conditions confirms both these trends.

With these findings in mind, we are now in a place to suggest design guidelines for mono-energetic proton radiography experiments at OMEGA. The parameters studied in more detail were chosen in part because the experimental designer has control over them. In general, experimentalists do not have much control over capsule conditions. This leaves only laser conditions that can be optimized for experimental applications. The scope of the design guidelines involves only optimizing proton yields from the backlighter. Other aspects such as source size cannot be improved, given the constraints of the sizes of targets and the energy of the lasers at OMEGA.

With the finding that laser asymmetry degrades performance and laser energy increases performance, experimentalists should try to use as many beams as possible (more laser energy) while keeping track of the asymmetry of the laser drive. Many experiments utilize as few beams as possible on the backlighter. If such a configuration is asymmetric enough, the D^3He backlighter could fail to produce enough yield for quality radiography.

Putting these guidelines to specific quantities for both number of beams and asymmetry is difficult and not entirely useful

because of natural spread in the DD and D^3He proton yields. With this caveat, we will still suggest a few bounds for consideration. Laser configurations with fewer than 18 beams should be avoided when the asymmetry measure is above 0.6. The combination of few beams and high asymmetry should be avoided whenever possible.

ACKNOWLEDGMENTS

This work was supported, in part, by the U.S. Department of Energy NNSA MIT Center-of-Excellence under Contract No. DE-NA0003868 and by the National Laser Users Facility under Contract No. DE-NA0003938. This report was prepared as an account of work sponsored by an agency of the United States Government. Neither the United States Government nor any agency thereof, nor any of their employees, makes any warranty, express or implied, or assumes any legal liability or responsibility for the accuracy, completeness, or usefulness of any information, apparatus, product, or process disclosed, or represents that its use would not infringe privately owned rights. Reference herein to any specific commercial product, process, or service by trade name, trademark, manufacturer, or otherwise does not necessarily constitute or imply its endorsement, recommendation, or favoring by the United States Government or any agency thereof. The views and opinions of authors expressed herein do not necessarily state or reflect those of the United States Government or any agency thereof.

DATA AVAILABILITY

Raw data were generated at OMEGA. Derived data supporting the findings of this study are available from the corresponding author upon reasonable request.

REFERENCES

- ¹C. K. Li *et al.*, *Rev. Sci. Instrum.* **77**, 10E725 (2006).
- ²C. K. Li *et al.*, *Phys. Rev. Lett.* **97**, 135003 (2006).
- ³A. B. Zylstra *et al.*, *Phys. Rev. Lett.* **114**, 215002 (2015).
- ⁴C. K. Li *et al.*, *Nat. Commun.* **7**, 13081 (2016).
- ⁵J. R. Rygg *et al.*, *Science* **319**, 1223 (2008).
- ⁶C. K. Li *et al.*, *Science* **327**, 1231 (2010).
- ⁷C. K. Li *et al.*, *Phys. Rev. Lett.* **123**, 055002 (2019).
- ⁸A. F. A. Bott *et al.*, *J. Plasma Phys.* **83**, 905830614 (2017).
- ⁹N. L. Kugland, D. D. Ryutov, C. Plechaty, J. S. Ross, and H.-S. Park, *Rev. Sci. Instrum.* **83**, 101301 (2012).
- ¹⁰F. H. Séguin *et al.*, *Rev. Sci. Instrum.* **74**, 975 (2003).
- ¹¹V. Y. Glebov *et al.*, *Rev. Sci. Instrum.* **75**, 3559 (2004).
- ¹²H.-S. Bosch and G. M. Hale, *Nucl. Fusion* **32**, 611 (1992).
- ¹³S. Skupsky *et al.*, *J. Appl. Phys.* **66**, 3456 (1989).
- ¹⁴J. J. MacFarlane, *J. Quant. Spectrosc. Radiat. Transfer* **81**, 287 (2003).
- ¹⁵SciPy 1.0 Contributors *et al.*, *Nat. Methods* **17**, 261 (2020).
- ¹⁶K. Levenberg, *Q. Appl. Math.* **2**, 164 (1944).